Advances in Applied Mathematics and Mechanics
Adv. Appl. Math. Mech., Vol. **9**, No. 2, pp. 250-271

DOI: 10.4208/aamm.2014.m888
April 2017

New Conservative Finite Volume Element Schemes for the Modified Regularized Long Wave Equation

Jinliang Yan[1,2], Ming-Chih Lai[3], Zhilin Li[4] and Zhiyue Zhang[1,*]

[1] *Jiangsu Key Laboratory for NSLSCS, School of Mathematical Sciences, Nanjing Normal University, Nanjing, Jiangsu 210023, China*
[2] *Wuyi University, Department of Mathematics and Computer, Wuyishan, Fujian 354300, China*
[3] *Department of Applied mathematics, National Chiao Tung University, Taiwan*
[4] *Center for Research in Scientific Computation, Department of Mathematics, North Carolina State University, Raleigh, North Carolina 27695-8205, USA*

Received 17 December 2014; Accepted (in revised version) 19 April 2016

Abstract. In this paper, we propose a new energy-preserving scheme and a new momentum-preserving scheme for the modified regularized long wave equation. The proposed schemes are designed by using the discrete variational derivative method and the finite volume element method. For comparison, we also propose a finite volume element scheme. The conservation properties of the proposed schemes are analyzed and we find that the energy-preserving scheme can precisely conserve the discrete total mass and total energy, the momentum-preserving scheme can precisely conserve the discrete total mass and total momentum, while the finite volume element scheme merely conserve the discrete total mass. We also analyze their linear stability property using the Von Neumann theory and find that the proposed schemes are unconditionally linear stable. Finally, we present some numerical examples to illustrate the effectiveness of the proposed schemes.

AMS subject classifications: 65M99, 70H06, 74J35, 74S99
Key words: Energy, momentum, mass, finite volume element method, MRLW equation.

1 Introduction

In this paper, we consider the following initial boundary value problem

$$\begin{cases} u_t+u_x+\kappa u^2u_x-\mu u_{xxt}=0, \quad a\le x\le b, \quad t>0, \\ u(x,0)=u_0(x), \\ \dfrac{\partial^j u}{\partial x^j}\Big|_{x=a}=\dfrac{\partial^j u}{\partial x^j}\Big|_{x=b}, \quad j=0,1,2, \end{cases} \tag{1.1}$$

*Corresponding author.
Email: zhangzhiyue@njnu.edu.cn (Z. Y. Zhang)

 ©2017 Global Science Press

https://doi.org/10.4208/aamm.2014.m888 Published online by Cambridge University Press

where κ and μ are positive constants. The equation is also known as modified regularized long wave (MRLW) equation. In fact, MRLW equation is a special case of generalized regularized long wave (GRLW) equation which has the form

$$u_t+u_x+\kappa u^p u_x-\mu u_{xxt}=0, \tag{1.2}$$

where p is a positive integer. MRLW equation is an important equation which has many applications in sciences, for example, drift waves in plasma, the Rossby waves in rotating fluids, the transverse waves in shallow water, pressure waves in liquid-gas bubble mixtures, and so on [1,2]. Their solutions are a kind of solitary waves named solitons whose amplitudes, shapes and velocities are not affected by collision.

In this paper, the discrete variational derivative method (DVDM) [3] and the finite volume element method (FVEM) are applied to study the conservative schemes of MRLW equation. The DVDM is a method of designing special numerical schemes that retain the conservation/dissipation properties of the original partial differential equations (PDEs). In this aspect, various numerical schemes were proposed and studied in the literature. For example, Furihata and Mori [4] has proposed a stable finite difference scheme for the Cahn-Hilliard equation. Koide and Furihata [6] has used the DVDM to design four conservative schemes for the regularized long wave equation. Further, Matsuo and Furihata [7] has extended the general studies to complex-valued PDEs such as the nonlinear Schrödinger equation. Recently, the method has been extended in various ways, such as Yaguchi, Matsuo and Sugihara [8] has extended the method to nonuniform grids. Matsuo and Kuramae [9,10] have further developed an alternating DVDM, and so on.

The FVEM, as a type of important numerical tool for solving differential equations, has a long history. This method is also known as a box method in some early references [11,12], or known as a generalized difference method [13,14] in China. This method has been widely used in several engineering fields, such as fluid mechanics, heat and mass transfer and petroleum engineering. Perhaps the most important property of FVEM is that it can preserve the conservation laws (mass, momentum and heat flux) on each computational element. This important property, in combination with adequate accuracy and ease of implementation, has attracted many researchers to do research in this field [15–20].

Li and Vu-Quoc [21] once said that "in some areas, the ability to preserve some invariant properties of the original differential equation is a criterion to judge the success of a numerical simulation". Thus, the main purpose of this paper is to study the conservative schemes of the MRLW equation. For MRLW equation, researchers have done a lot of work, for instance, Gardner et al. [22] has used the cubic B-spline finite element method to solve the MRLW equation. Durán and López-Marcos [5] has investigated some advantages of conservative numerical methods. Khalifa et al. [23,24] have used the finite difference method and collocation method with cubic B-splines to solve the MRLW equation. Raslan [25] has proposed a new algorithm based on the collocation method to solve the MRLW equation. Cai [26] has proposed a multi-symplectic explicit scheme for MRLW

https://doi.org/10.4208/aamm.2014.m888 Published online by Cambridge University Press

equation, and so on. In this paper, we propose three conservative finite volume element schemes for the MRLW equation.

To our knowledge, the MRLW equation satisfies only three conservation laws given by [28]:

$$M=\int_a^b u dx, \tag{1.3a}$$

$$K=\frac{1}{2}\int_a^b \left\{u^2+\mu\left(\frac{\partial u}{\partial x}\right)^2\right\}dx, \tag{1.3b}$$

$$J=\int_a^b \left(\frac{\kappa}{12}u^4+\frac{1}{2}u^2\right)dx, \tag{1.3c}$$

which correspond to conservation of mass, momentum and energy, respectively.

This work is devoted to the design of conservative finite volume element schemes for the MRLW equation. We first construct the energy-preserving and momentum-preserving finite volume element schemes using the DVDM and the FVEM. At last, for comparison, we derive the standard finite volume element scheme by using implicit midpoint rule in time. The schemes are obtained by using the linear finite volume element method in space and finite difference method in time so that the generated schemes are of second-order accuracy in space and time.

The paper is organized as follows. In Section 2, notation and preliminaries associated with FVEM are defined. In Section 3, new conservative finite volume element schemes are proposed and analyzed rigorously. In Section 4, linear stability of the proposed schemes are presented. In Section 5, numerical results are reported. Finally, some concluding remarks are drawn in Section 6.

2 Notation and preliminaries

In this section, we define some notations employed in this paper.

Discretize the interval $I=[a,b]$ into a grid T_h with nodes

$$a=x_0<x_1<x_2<\cdots<x_{n-1}<x_n=b,$$

where $h=x_i-x_{i-1}$ denotes the length of the element I_i and $h=\frac{b-a}{N}$. Denote $T_h=\{I_i: I_i=[x_{i-1},x_i],\ i=1,2,\cdots,N\}$. Next we place a dual grid T_h^* with nodes

$$a=x_0<x_{1/2}<x_{3/2}<\cdots<x_{n-1/2}<x_N=b,$$

where $x_{i-1/2}=(x_{i-1}+x_i)/2$, $i=1,2,\cdots,N$. $I_0^*=[x_0,x_{1/2}]$, $I_i^*=[x_{i-1/2},x_{i-1/2}]$ $(i=1,2,\cdots,N-1)$ and $I_N^*=[x_{N-1/2},x_N]$ denote the dual element. The trial space U_h is taken as the linear element space with respect to T_h. The basis function with respect to x_i is

$$\phi_i(x)=\begin{cases} 1-h^{-1}|x-x_i|, & x_{i-1}\le x\le x_i,\\ 0, & \text{elsewhere.}\end{cases}$$

https://doi.org/10.4208/aamm.2014.m888 Published online by Cambridge University Press

The functions $\{\phi_i(x): i=1,2,\cdots,N\}$ form a basis of U_h and any $u_h \in U_h$ has the following expression

$$u_h = \sum_{i=1}^{N} u_i \phi_i(x),$$

where $u_i = u_h(x_i,t)$. Thus on the element I_i, we have

$$u_h = u_{i-1}(1-\xi) + u_i \xi, \tag{2.1a}$$

$$u_h' = (u_i - u_{i-1})/h, \quad x \in I_i, \quad i=1,2,\cdots,N, \tag{2.1b}$$

where $\xi = (x - x_{i-1})/h$.

Accordingly we choose the test function space V_h as the piecewise constant function (step function) space. The basis functions of V_h are

$$\psi_j(x) = \begin{cases} 1, & x_{j-1/2} \le x \le x_{j+1/2}, \\ 0, & \text{elsewhere}, \end{cases}$$

where $j=1,2,\cdots,N$. Any $v_h \in V_h$ has the form

$$v_h = \sum_{i=1}^{N} v_i \psi_i(x),$$

where $v_i = v_h(x_i,t)$. The numerical solution is denoted by $U_k^{(m)} = u(k\Delta x, m\Delta t)$, where Δx is the space mesh size, Δt is the time mesh size. For the MRLW equation, we adopt the following periodic boundary conditions

$$\frac{\partial^j u}{\partial x^j}\Big|_{x=a} = \frac{\partial^j u}{\partial x^j}\Big|_{x=b}, \quad (j=0,1,2). \tag{2.2}$$

And the corresponding discrete periodic boundary condition is defined as

$$U_k^{(m)} = U_{k \bmod N}^{(m)}, \quad \forall k \in \mathbb{Z}, \tag{2.3}$$

which implies that $U^{(m)} \in \mathbb{S}_N$, and

$$\mathbb{S}_N \overset{d}{=} \left\{ (U_k \in \mathbb{R})_{k\in\mathbb{Z}} \middle| U_k = U_{k \bmod N} \right\}.$$

3 Numerical schemes

In this section, we propose the conservative finite volume element schemes, and further analyze their conservation properties.

https://doi.org/10.4208/aamm.2014.m888 Published online by Cambridge University Press

3.1 Discrete variational derivative method

In order to derive the proposed schemes, we first define the "free energy" or "local energy" of Eq. (1.1) as

$$G(u,u_x)=\frac{\kappa}{12}u^4+\frac{1}{2}u^2.$$

We call its spatial integration

$$J(u)=\int_a^b G(u,u_x)dx$$

the "global energy". Thus Eq. (1.1) can be rewritten as

$$(1-\mu\partial_x^2)u_t=-\frac{\partial}{\partial x}\Big(\frac{\delta G}{\delta u}\Big), \tag{3.1}$$

where $\partial_x^2=\partial^2/\partial x^2$, and $\delta G/\delta u$ is the (first) variational derivative of $G(u,u_x)$ defined by

$$\frac{\delta G}{\delta u}=\frac{\partial G}{\partial u}-\frac{\partial}{\partial x}\Big(\frac{\partial G}{\partial u_x}\Big). \tag{3.2}$$

Then we present a scheme of "local energy"

$$G_{d,k}(U^{(m)})=\frac{\kappa}{12}(U_k^{(m)})^4+\frac{1}{2}(U_k^{(m)})^2,$$

where $U_k^{(m)}\simeq u(a+kh,m\Delta t)$, $k=0,1,\cdots,N$, $m=0,1,2,\cdots$.

At last, we can obtain a discrete scheme of Eq. (3.2) by the following difference:

$$\begin{aligned}
&\sum_{k=0}^{N}{}''\Big[G_{d,k}(U^{(m+1)})-G_{d,k}(U^{(m)})\Big]\Delta x\\
=&\sum_{k=0}^{N}{}''\Big\{\frac{\kappa}{12}\Big[(U_k^{(m+1)})^4-(U_k^{(m)})^4\Big]+\frac{1}{2}\Big[(U_k^{(m+1)})^4-(U_k^{(m)})^4\Big]\Big\}\Delta x\\
=&\sum_{k=0}^{N}{}''\Big\{\frac{\kappa}{12}\Big[(U_k^{(m+1)})^2+(U_k^{(m)})^2\Big](U_k^{(m+1)}+U_k^{(m)})(U_k^{(m+1)}-U_k^{(m)})\\
&\qquad+\frac{1}{2}(U_k^{(m+1)}+U_k^{(m)})(U_k^{(m+1)}-U_k^{(m)})\Big\}\Delta x\\
=&\sum_{k=0}^{N}{}''\Big\{\Big[\frac{\kappa}{12}\Big((U_k^{(m+1)})^2+(U_k^{(m)})^2\Big)+\frac{1}{2}\Big](U_k^{(m+1)}+U_k^{(m)})\Big\}(U_k^{(m+1)}-U_k^{(m)})\Delta x,
\end{aligned} \tag{3.3}$$

where

$$\sum_{k=0}^{N}{}''f_k\overset{d}{\equiv}\frac{1}{2}f_0+f_1+\cdots+f_{N-1}+\frac{1}{2}f_N$$

is the trapezoidal rule.

https://doi.org/10.4208/aamm.2014.m888 Published online by Cambridge University Press

From Eq. (3.3), we have

$$\frac{\delta G_d}{\delta(U^{(m+1)},U^{(m)})_k}=\Big\{\frac{\kappa}{12}\Big[(U_k^{(m+1)})^2+(U_k^{(m)})^2\Big]+\frac{1}{2}\Big\}(U_k^{(m+1)}+U_k^{(m)}).$$

On the other hand, in order to derive the momentum-preserving scheme, we propose another scheme of $\frac{\delta G}{\delta u}$

$$\frac{\delta G_d}{\delta(U_+^{(m)},U_-^{(m)})_k}=\Big\{\frac{\kappa}{12}\Big[(U_+^{(m)})_k^2+(U_-^{(m)})_k^2\Big]+\frac{1}{2}\Big\}\big[(U_+^{(m)})_k+(U_-^{(m)})_k\big],$$

where

$$(U_+^{(m)})_k\overset{d}{=}\frac{1}{2}(U_{k+1}^{(m+1)}+U_{k+1}^{(m)}),\quad (U_-^{(m)})_k\overset{d}{=}\frac{1}{2}(U_{k-1}^{(m+1)}+U_{k-1}^{(m)}),\quad k\in\mathbb{Z},\quad m=0,1,\cdots.$$

3.2 Concrete form of the proposed schemes

In order to derive the semi-discrete scheme of (3.1), we can approximate the unknown solution $u(x,t)$ of partial differential equation as follows:

$$u(x,t)\simeq U^{(m)}(x)=\sum_{i=1}^{N}u^{(m)}(x)\phi_i(x),\quad \phi_i(x)\in H^1(\Omega).$$

Then let us derive the semi-discrete conservative finite volume element schemes of (3.1). First, use any function $\psi\in V_h$ to multiply Eq. (3.1) and integrate it on $[a,b]$, we obtain

$$\big((1-\mu\partial_x^2)u_t,\psi\big)=-\Big(\frac{\partial}{\partial x}\Big(\frac{\delta G}{\delta u}\Big),\psi\Big),$$

where $(\cdot,\cdot)$ denotes the inner product of $L^2([a,b])$.

Then, we can obtain the following energy-preserving finite volume element scheme of Eq. (1.1):

$$\big((1-\mu\partial_x^2)\delta_m^+U^{(m)},\psi_i\big)=-\Big(\frac{\partial}{\partial x}\Big(\frac{\delta G_d}{\delta(U^{(m+1)},U^{(m)})}\Big),\psi_i\Big),\quad i=1,2,\cdots,N,\tag{3.4}$$

where $\delta_m^+U^{(m)}=(U^{(m+1)}-U^{(m)})/\Delta t$, and

$$\frac{\delta G_d}{\delta(U^{(m+1)},U^{(m)})}=\Big\{\frac{\kappa}{12}\Big[(U^{(m+1)})^2+(U^{(m)})^2\Big]+\frac{1}{2}\Big\}(U^{(m+1)}+U^{(m)})$$

is a semi-discrete formulation of $\delta G/\delta u$.

Similarly, we also have the following momentum-preserving finite volume element scheme of Eq. (1.1):

$$\big((1-\mu\partial_x^2)\delta_m^+U^{(m)},\psi_j\big)=-\Big(\frac{\partial}{\partial x}\Big(\frac{\delta G_d}{\delta(U_+^{(m)},U_-^{(m)})}\Big),\psi_j\Big),\quad j=1,2,\cdots,N,\tag{3.5}$$

https://doi.org/10.4208/aamm.2014.m888 Published online by Cambridge University Press

where

$$\frac{\delta G_d}{\delta(U_+^{(m)},U_-^{(m)})}=\left\{\frac{\kappa}{12}\left[(U_+^{(m)})^2+(U_-^{(m)})^2\right]+\frac{1}{2}\right\}(U_+^{(m)}+U_-^{(m)})$$

is another semi-discrete formulation of $\delta G/\delta u$.

For comparison, we also construct the following standard finite volume element scheme:

$$\begin{aligned}&\left((1-\mu\partial_x^2)\delta_m^+U^m,\psi_k\right)\\&=-\left(\frac{\partial}{\partial x}\left[\frac{\kappa}{3}\left(\frac{U^{(m)}+U^{(m+1)}}{2}\right)^3+\left(\frac{U^{(m)}+U^{(m+1)}}{2}\right)\right],\psi_k\right),\quad k=1,2,\cdots,N.\end{aligned}\tag{3.6}$$

Remark 3.1. We can derive the fully discrete linear element difference schemes by choosing the trial and the test function spaces as linear finite element and piecewise constant function spaces respectively.

In this paper, we use the following fixed-point iteration method to solve Eq. (1.1):

Step 1 Choose tol:=1, eps:=10^{-14}, $U^{(0)}:=U_0$;
Input coefficient matrix $\mathbb{A}$ and $\mathbb{B}$;
Set $k:=0$, $n:=1$.

Step 2 While tol> eps Compute the right hand side $g:=F^{(k)}$ of proposed schemes.

Step 3 Compute $U^{(k+1)}\in S_N$ given by

$$\mathbb{A}\,U^{(k+1)}:=\mathbb{B}U^{(k)}+g.$$

Step 4 Compute tol:=$\|U^{(k+1)}-U^{(0)}\|$, $U^{(0)}:=U^{(k+1)}$.

Step 5 The stopping criterion:
If $\|U^{(k+1)}-U^{(0)}\|<$ eps
then stop ($U^{(k+1)}$ is the solution), $k:=k+1$, go to Step 1.
else $n:=n+1$, go to Step 2.

3.3 Conservation properties of the proposed schemes

In the sequel, we study the conservation properties of the MRLW equation, which are mentioned in the introduction, namely,

$$\frac{d}{dt}M(u(\cdot,t))=0,\tag{3.7a}$$

$$\frac{d}{dt}K(u(\cdot,t))=0,\tag{3.7b}$$

$$\frac{d}{dt}J(u(\cdot,t))=0.\tag{3.7c}$$

Eq. (3.7) respectively corresponds mass, momentum and energy conservation law. Under the periodic boundary condition (2.2), we can easily prove it [3,6], for simplicity, here we only give the associated result.

https://doi.org/10.4208/aamm.2014.m888 Published online by Cambridge University Press

Proposition 3.1. Let u be the solution of Eq. (1.1), then the total mass M in (1.3a) is constant, that is

$$\frac{d}{dt}\int_a^b u dx = 0.$$

Proposition 3.2. Let u be the solution of Eq. (1.1), then the total momentum K in (1.3b) is constant, that is

$$\frac{1}{2}\frac{d}{dt}\int_a^b \left[u^2+\mu(u_x)^2\right]dx = 0.$$

Proposition 3.3. Let u be the solution of Eq. (1.1), then the total energy J in (1.3c) is constant, that is

$$\frac{d}{dt}\int_a^b G(u,u_x)dx = 0,$$

where

$$G(u,u_x) \overset{d}{=} \frac{\kappa}{12}u^4+\frac{1}{2}u^2.$$

Now we start to study the discrete conservation laws of (3.4)-(3.6). Firstly, for the semi-discrete scheme (3.4), we have the following discrete mass and energy conservation properties:

Theorem 3.1 (Discrete mass conservation law)**.** *Let $U^{(m)}$ be the solution of Eq.* (3.4)*, then the discrete total mass M is constant, namely*

$$\int_a^b U^{(m)}dx = const.$$

Proof. We will see

$$\begin{aligned}
&\frac{1}{\Delta t}\left[M(U^{(m+1)})-M(U^{(m)})\right]\\
=&\frac{1}{\Delta t}\int_a^b (U^{(m+1)}-U^{(m)})dx = \int_a^b \frac{U^{(m+1)}-U^{(m)}}{\Delta t}dx\\
=&\int_a^b \frac{\partial}{\partial x}\Big(\mu\frac{\partial}{\partial x}(\delta_m^+ U^{(m)})-\frac{\delta G_d}{\delta(U^{(m+1)},U^{(m)})}\Big)dx\\
=&\Big[\mu\frac{\partial}{\partial x}(\delta_m^+ U^{(m)})-\frac{\delta G_d}{\delta(U^{(m+1)},U^{(m)})}\Big]_{x=a}^{b} = 0.
\end{aligned}$$

Thus, the theorem is proved. □

Theorem 3.2 (Discrete energy conservation law)**.** *Let $U^{(m)}$ be the solution of Eq.* (3.4)*, then the discrete total energy J is constant, namely*

$$\int_a^b G_d(U^{(m)})dx = const,$$

https://doi.org/10.4208/aamm.2014.m888 Published online by Cambridge University Press

where

$$G_d(U^{(m)})=\frac{\kappa}{12}(U^{(m)})^4+\frac{1}{2}(U^{(m)})^2.$$

Proof. It holds

$$\begin{aligned}
&\frac{1}{\Delta t}\Big[J(U^{(m+1)})-J(U^{(m)})\Big]\\
=&\frac{1}{\Delta t}\int_a^b\Big[G_d(U^{(m+1)})-G_d(U^{(m)})\Big]dx=\int_a^b\frac{\delta G_d}{\delta(U^{(m+1)},U^{(m)})}\delta_m^+U^{(m)}dx\\
=&\int_a^b\Big\{\Big(\frac{\delta G_d}{\delta(U^{(m+1)},U^{(m)})}-\mu\frac{\partial}{\partial x}(\delta_m^+U^{(m)})\Big)\delta_m^+U^{(m)}+\mu\frac{\partial}{\partial x}(\delta_m^+U^{(m)})\delta_m^+U^{(m)}\Big\}dx\\
=&\int_a^b\Big\{-\Big(\mu\frac{\partial}{\partial x}(\delta_m^+U^{(m)})-\frac{\delta G_d}{\delta(U^{(m+1)},U^{(m)})}\Big)\frac{\partial}{\partial x}\Big(\mu\frac{\partial}{\partial x}(\delta_m^+U^{(m)})-\frac{\delta G_d}{\delta(U^{(m+1)},U^{(m)})}\Big)\\
&+\frac{\mu}{2}\frac{\partial}{\partial x}(\delta_m^+U^{(m)})^2\Big\}dx\\
=&\frac{1}{2}\Big[-\Big(\mu\frac{\partial}{\partial x}(\delta_m^+U^{(m)})-\frac{\delta G_d}{\delta(U^{(m+1)},U^{(m)})}\Big)^2+\mu(\delta_m^+U^{(m)})^2\Big]_{x=a}^b=0.
\end{aligned}$$

So, we have completed the proof. □

Secondly, for the semi-discrete scheme (3.5), we have the following discrete mass and momentum conservation properties:

Theorem 3.3 (Discrete mass conservation law)**.** *Let $U^{(m)}$ be the solution of Eq.* (3.5)*, then the discrete total mass M is constant, namely*

$$\int_a^b U^{(m)}dx=const.$$

Theorem 3.4 (Discrete momentum conservation law)**.** *Let $U^{(m)}$ be the solution of Eq.* (3.5)*, then the discrete total momentum K is constant, namely*

$$\frac{1}{2}\int_a^b\Big[(U^{(m)})^2+\mu(U_x^{(m)})^2\Big]dx=const.$$

Proof. We will prove

$$\begin{aligned}
&\frac{1}{\Delta t}\Big[K(U^{(m+1)})-K(U^{(m)})\Big]\\
=&\frac{1}{2\Delta t}\Big\{\int_a^b\Big[(U^{(m+1)})^2+\mu(U_x^{(m+1)})^2\Big]dx-\int_a^b\Big[(U^{(m)})^2+\mu(U_x^{(m)})^2\Big]dx\Big\}\\
=&\frac{1}{2\Delta t}\Big\{\int_a^b\Big[(U^{(m+1)})^2-(U^{(m)})^2\Big]dx+\mu\int_a^b\Big[(U_x^{(m+1)})^2-(U_x^{(m)})^2\Big]dx\Big\}
\end{aligned}$$

https://doi.org/10.4208/aamm.2014.m888 Published online by Cambridge University Press

$$
\begin{aligned}
&=\int_a^b \Big\{ \frac{U^{(m+1)}+U^{(m)}}{2} \frac{U^{(m+1)}-U^{(m)}}{\Delta t} + \mu \frac{\partial}{\partial x}\Big(\frac{U^{(m+1)}+U^{(m)}}{2}\Big) \frac{\partial}{\partial x}\Big(\frac{U^{(m+1)}-U^{(m)}}{\Delta t}\Big) \Big\} dx \\
&=\int_a^b \Big(\frac{U^{(m+1)}+U^{(m)}}{2}\Big) \delta_m^+ U^{(m)} dx + \mu \int_a^b \frac{\partial}{\partial x}\Big(\frac{U^{(m+1)}+U^{(m)}}{2}\Big) \frac{\partial}{\partial x}\big(\delta_m^+ U^{(m)}\big) dx \\
&=\int_a^b \Big(\frac{U^{(m+1)}+U^{(m)}}{2}\Big) \delta_m^+ U^{(m)} dx - \mu \int_a^b \Big(\frac{U^{(m+1)}+U^{(m)}}{2}\Big) \frac{\partial^2}{\partial x^2}\big(\delta_m^+ U^{(m)}\big) dx \\
&=\int_a^b \Big(\frac{U^{(m+1)}+U^{(m)}}{2}\Big) \Big[\delta_m^+ U^{(m)} - \mu \frac{\partial^2}{\partial x^2}\big(\delta_m^+ U^{(m)}\big)\Big] dx \\
&=-\int_a^b \Big(\frac{U^{(m+1)}+U^{(m)}}{2}\Big) \frac{\partial}{\partial x}\Big(\frac{\delta G_d}{\delta(U_+^{(m)}, U_-^{(m)})}\Big) dx \\
&=\int_a^b \frac{\partial}{\partial x}\Big(\frac{U^{(m+1)}+U^{(m)}}{2}\Big) \Big(\frac{\delta G_d}{\delta(U_+^{(m)}, U_-^{(m)})}\Big) dx \\
&=\int_a^b \frac{\partial}{\partial x} G_d(U^{(m)}) dx = \big[G_d(U^{(m)})\big]_{x=a}^b = 0.
\end{aligned} \tag{3.8}
$$

Thus, we have completed the proof. □

Remark 3.2. In the above equations, integration by parts formula and discrete periodic boundary condition (2.3) are used.

At last, for the semi-discrete scheme (3.6), we have the following discrete mass conservation property:

Theorem 3.5 (Discrete mass conservation law)**.** *Let $U^{(m)}$ be the solution of Eq.* (3.6)*, then the discrete total mass M is constant, namely*

$$\int_a^b U^{(m)} dx = const.$$

The conservation property can also be proved like Theorem 3.1 based on the periodic boundary condition (2.3).

4 Linear stability analysis

In this section, we consider the linear stability of the proposed schemes, here we apply the Von Neumann stability theory to the proposed schemes.

Theorem 4.1. *The energy-preserving scheme* (3.4)*, the momentum-preserving scheme* (3.5) *and the standard finite volume element scheme* (3.6) *are unconditionally linear stable.*

https://doi.org/10.4208/aamm.2014.m888 Published online by Cambridge University Press

Proof. Firstly, from Eq. (3.4), we get the following energy-preserving finite volume element scheme:

$$\begin{aligned}&\alpha_1 U_{k-1}^{(m+1)}+\alpha_2 U_k^{(m+1)}+\alpha_3 U_{k+1}^{(m+1)}\\ =&\alpha_3 U_{k-1}^{(m)}+\alpha_2 U_k^{(m)}+\alpha_1 U_{k+1}^{(m)}\\ &+\alpha_4\Big\{\big[(U_{k-1}^{(m+1)})^2+(U_{k-1}^{(m)})^2\big](U_{k-1}^{(m+1)}+U_{k-1}^{(m)})\\ &-\big[(U_{k+1}^{(m+1)})^2+(U_{k+1}^{(m)})^2\big](U_{k+1}^{(m+1)}+U_{k+1}^{(m)})\Big\},\end{aligned}\tag{4.1}$$

where

$$\alpha_1=-24\mu-6\Delta th,\qquad \alpha_2=24h^2+48\mu,\tag{4.2a}$$

$$\alpha_3=6\Delta th-24\mu,\qquad \alpha_4=\kappa\Delta th,\tag{4.2b}$$

and $k=0,1,\cdots,N$.

For the stability analysis, we consider the linear version of the proposed scheme (4.1), which can be given as

$$\begin{aligned}&\alpha_1 U_{k-1}^{(m+1)}+\alpha_2 U_k^{(m+1)}+\alpha_3 U_{k+1}^{(m+1)}\\ =&\alpha_3 U_{k-1}^{(m)}+\alpha_2 U_k^{(m)}+\alpha_1 U_{k+1}^{(m)}\\ &+\alpha_4 C(U_{k-1}^{(m+1)}+U_{k-1}^{(m)}-U_{k+1}^{(m+1)}-U_{k+1}^{(m)}),\end{aligned}\tag{4.3}$$

where

$$C=\max_{0\le k\le N}\{(U_k^{(m+1)})^2+(U_k^{(m)})^2\}.$$

To apply Von Neumann method, we assume that the solution of (4.1) is

$$U_j^m=V^m e^{i\alpha jh},\tag{4.4}$$

where V, α are constants, substituting (4.4) into (4.3), we have

$$(\beta_1+i\beta_2)V^{m+1}=(\beta_1-i\beta_2)V^m,\tag{4.5}$$

where

$$\beta_1=\alpha_1\cos(\alpha h)+\alpha_2+\alpha_3\cos(\alpha h),\quad \beta_2=\alpha_3\sin(\alpha h)-\alpha_1\sin(\alpha h)+2\alpha_4 C\sin(\alpha h).\tag{4.6}$$

Thus Eq. (4.5) can be written as

$$V^{m+1}=gV^m,$$

where

$$g=\frac{\beta_1-i\beta_2}{\beta_1+i\beta_2},$$

is growth factor, and the modulus of $|g|$ is 1, therefore the linearized scheme (3.4) is unconditionally stable. Similarly, we can also prove the scheme (3.5) and the scheme (3.6) are also unconditionally linear stable. □

https://doi.org/10.4208/aamm.2014.m888 Published online by Cambridge University Press

5 Numerical experiments

In this section, we will consider the following three test problems: the propagation of single solitary wave, the interaction of two and three solitary waves. Through these numerical examples, we validate the efficiency of the proposed schemes.

To measure the accuracy of the proposed schemes, we first define the following error norm and convergence rate:

$$L_\infty = \max_i |u_h(x_i) - u(x_i)|, \quad order = \log_2\Big(\frac{\|u_{2h}-u\|}{\|u_h-u\|}\Big), \tag{5.1}$$

where u_h and u denote the numerical solution with space step h and the exact solution, respectively.

On the other hand, in order to validate the conservation properties, we define the discrete conservation quantities corresponding to (1.3a)-(1.3c) as follows:

$$M_d(U^{(n)}) \simeq h \sum_{k=0}^{N-1}{}'' U_k^{(n)}, \tag{5.2a}$$

$$K_d(U^{(n)}) \simeq \frac{h}{2} \sum_{k=0}^{N-1}{}'' \Big[(U_k^{(n)})^2 + \mu \frac{(\delta_k^+ U_k^{(n)})^2 + (\delta_k^- U_k^{(n)})^2}{2}\Big], \tag{5.2b}$$

$$J_d(U^{(n)}) \simeq \frac{h}{2} \sum_{k=0}^{N-1}{}'' \Big[\frac{\kappa}{6}(U_k^{(n)})^4 + (U_k^{(n)})^2\Big], \tag{5.2c}$$

where $\delta_k^+ U_k^{(m)} = (U_{k+1}^{(m)} - U_k^{(m)})/h$, $\delta_k^- U_k^{(m)} = (U_k^{(m)} - U_{k-1}^{(m)})/h$.

In addition, we define the relative errors of the invariants as

$$RE^j = \log_{10}\Big(\frac{|E^j - E^0|}{|E^0|}\Big),$$

where E^j denotes the global quantities associated with the invariants on the j-th time level.

5.1 Single solitary wave

Let $\kappa = 1$, $\mu = 1$, then Eq. (1.1) becomes

$$u_t + u_x + u^2 u_x - u_{xxt} = 0. \tag{5.3}$$

Eq. (5.3) has the following solitary wave solution:

$$u(x,t) = \sqrt{6c}\,\mathrm{sech}\big(A(x-(c+1)t-x_0)\big), \tag{5.4}$$

https://doi.org/10.4208/aamm.2014.m888 Published online by Cambridge University Press

Table 1: The L_∞ error and convergence order of proposed schemes in space with $T=1$, $\Delta t=0.001$, $h=1/4$, $x_0=0$, $c=0.8$, $-20\le x\le 20$.

h	EFVEM	order	MFVEM	order	FVEM	order
1/2	0.050874	—	0.21866	—	0.050874	—
1/4	0.012715	2.0004	0.064581	1.7595	0.012715	2.0004
1/8	0.0031756	2.0014	0.016639	1.9565	0.0031755	2.0015
1/16	0.0007973	1.9938	0.0041981	1.9868	0.00079729	1.9938

Table 2: The L_∞ error and convergence order of proposed schemes in time with $T=1$, $h=1/40$, $x_0=0$, $c=0.8$, $-20\le x\le 20$.

Δt	EFVEM	order	MFVEM	order	FVEM	order
1/2	0.097781	—	0.093364	—	0.092965	—
1/4	0.027595	1.8251	0.026952	1.7925	0.026452	1.8133
1/8	0.0072277	1.9328	0.0074827	1.8488	0.0069498	1.9283
1/16	0.0019179	1.9140	0.0023914	1.6457	0.001849	1.9102

where $A=\sqrt{\frac{c}{(c+1)}}$, x_0 and c are constants. This solution corresponds to a solitary wave of amplitude $\sqrt{6c}$ and width A, initially located at $x=x_0$. Here c denotes the velocity of traveling wave, and the initial condition can be obtained by the exact solution

$$u(x,0)=\sqrt{6c}\operatorname{sech}\big(A(x-x_0)\big). \tag{5.5}$$

To compare the numerical results of three proposed schemes, we will choose $x_0=0$, $c=0.8$ in the following.

In order to measure the accuracy in space and time, we discretize the problem over the region $[-20,20]$ up to time $T=1$. Firstly, we choose a relatively small time step $\Delta t=0.001$ such that the error from the time discretization is negligible compared with those from the space. The results are presented in the Table 1, which clearly shows that the errors are halved when the space step is halved. In other words, the proposed schemes are second-order in space. Nevertheless, it is noted that the energy-preserving scheme and the standard finite volume element scheme have higher accuracy than the momentum-preserving scheme. The results also can be seen in the Fig. 1(a), the straight lines of three schemes are roughly parallel to the standard line $y=2x$.

Similarly, in order to investigate the accuracy in time, we choose a relatively small space step $h=1/40$ such that the error from the space discretization is negligible. The L_∞ errors and convergence orders are presented in Table 2, which shows that the proposed schemes are second-order in time, but the energy-preserving scheme and the standard finite volume element scheme have better stability than the momentum-preserving scheme, which also can be seen in Fig. 1(b), the straight line of momentum-preserving scheme curves downward. In addition, Table 3 list the results when $h=\Delta t$. The results clearly show that the proposed schemes are second-order in space and time, which can also be seen in Fig. 1(c).

https://doi.org/10.4208/aamm.2014.m888 Published online by Cambridge University Press

Table 3: The L_∞ error and convergence order of proposed schemes when $h=\Delta t$ and $T=1$, $-20\le x\le 20$.

$h=\Delta t$	EFVEM	order	MFVEM	order	FVEM	order
1/2	0.13562	—	0.26407	—	0.13164	—
1/4	0.039218	1.7900	0.085951	1.6193	0.038138	1.7873
1/8	0.010202	1.9427	0.023109	1.8951	0.0099353	1.9406
1/16	0.0025835	1.9815	0.0058952	1.9708	0.0025143	1.9824

Secondly, we perform a simulation with space step $h=1/4$ and time step $\Delta t=0.01$ for a single solitary wave over the region $[-20,20]$ up to time $T=1$. Fig. 2(a) presents the numerical results of the energy-preserving scheme and shows that the solitary wave moves to the right at a constant speed and almost unchanged amplitude as time progresses, as is expected. We also calculate the relative errors of the invariants evaluated along the numerical solution with respect to the the conserved quantities at $t=0$. Fig. 2(b) presents the conservation properties of the energy-preserving scheme and shows that it can precisely conserve the discrete mass and energy to within the machine precision. On the other hand, Fig. 3 presents the conservation properties of the momentum-preserving scheme and the finite volume element scheme and shows that the momentum-preserving scheme can precisely conserve the discrete mass and momentum, and the finite volume element scheme only can precisely conserve the discrete mass to within the machine precision. So the energy-preserving scheme and the momentum-preserving scheme have better conservation properties than the standard finite volume element scheme.

Fig. 4 presents the numerical solution and the exact solution of the energy-preserving scheme and the momentum-preserving scheme in the time interval $[0,1]$. Fig. 5 presents the errors associated with the proposed methods and shows that the energy-preserving scheme have higher accuracy than the momentum-preserving scheme.

Thirdly, in order to study the long-time conservation properties of the proposed

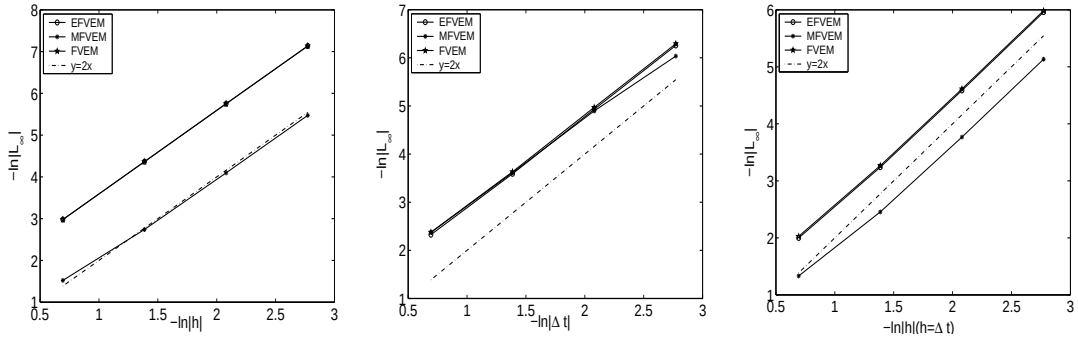


Figure 1: The convergence order of the proposed schemes. (a): convergence order in space; (b): convergence order in time; (c): convergence order when $h=\Delta t$.

https://doi.org/10.4208/aamm.2014.m888 Published online by Cambridge University Press

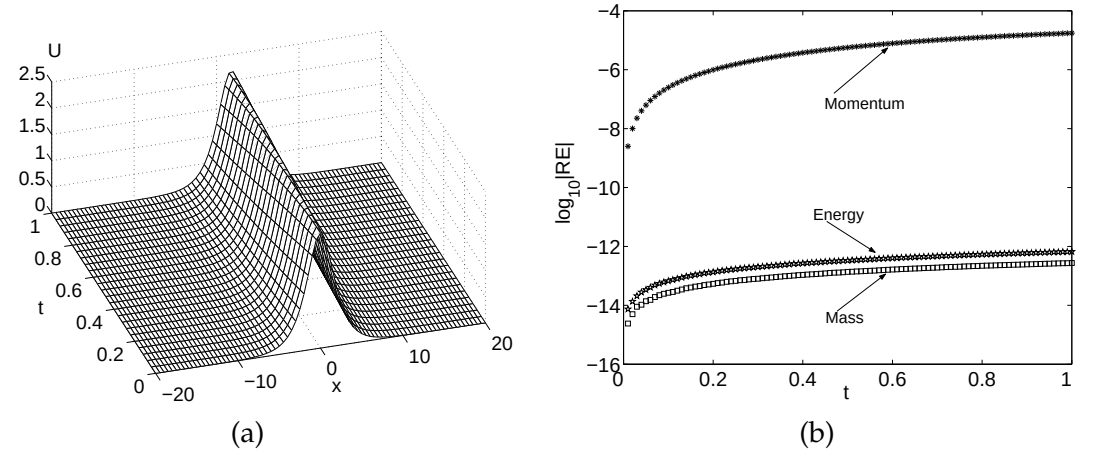


Figure 2: The numerical results of energy-preserving scheme with $T=1$, $\Delta t=0.01$, $h=1/4$, $c=0.8$, $x_0=0$. (a): the numerical solution at $T=1$; (b): the relative errors of invariants.

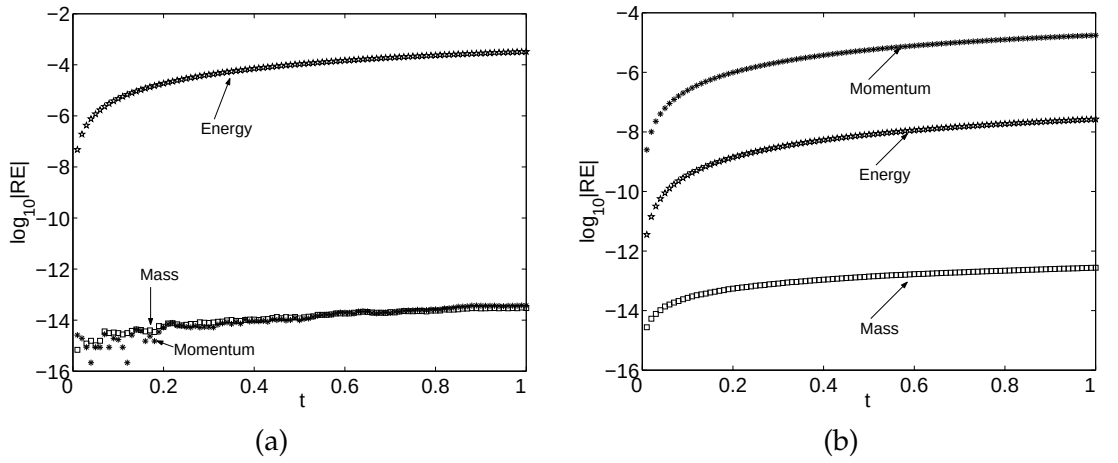
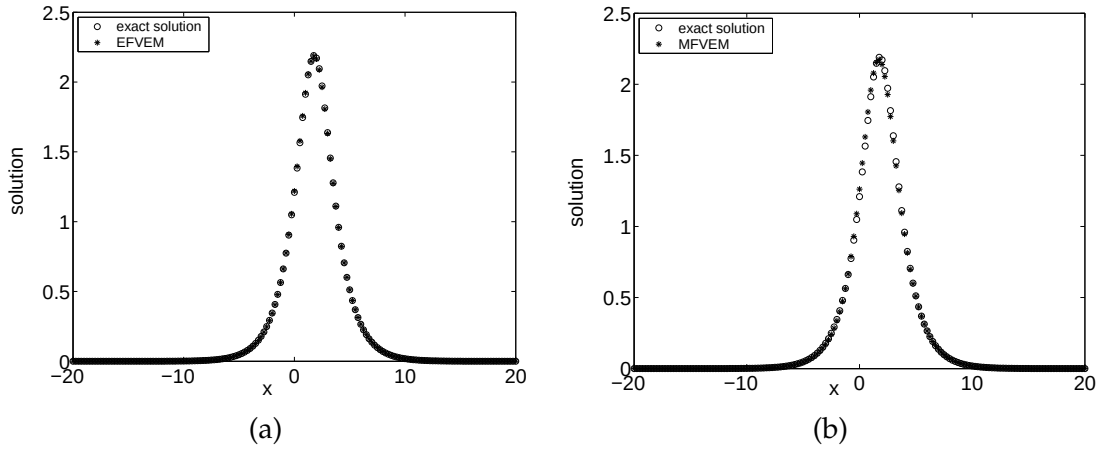


Figure 3: The relative errors of invariants for momentum-preserving scheme and finite volume element scheme with $T=1$, $\Delta t=0.01$, $h=1/4$, $c=0.8$, $x_0=0$. (a): momentum-preserving scheme; (b): finite volume element scheme.

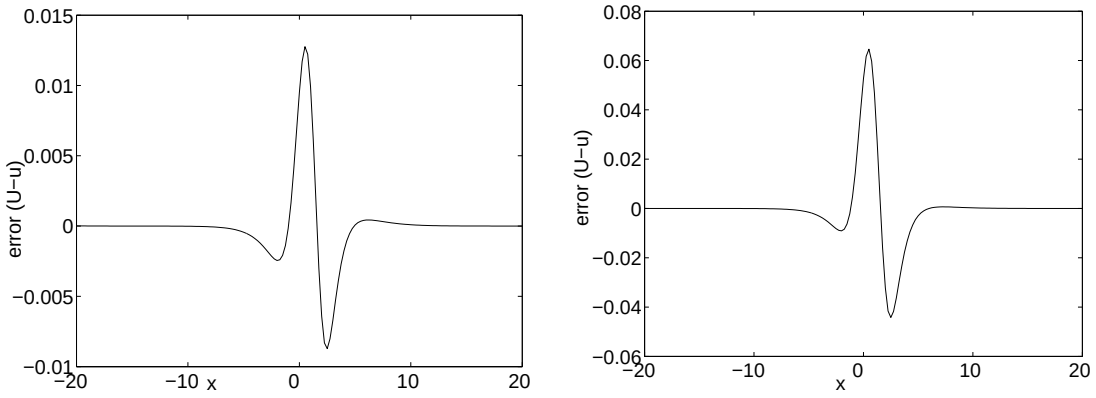
schemes, we also perform a simulation with space step $h=1/4$ and time step $\Delta t=0.1$ for a solitary wave over the region $[-20,20]$ up to time $T=1000$. Fig. 6 presents the numerical results of the energy-preserving scheme in the time interval $[0,1000]$. The solitary wave propagates towards the right at a constant speed and almost unchanged amplitude. Moreover, the scheme reveals very good long-time conservation properties in preserving the discrete mass and energy. On the other hand, Fig. 7 presents the conservation properties of the momentum-preserving scheme and the finite volume element scheme and also reveals very good long-time conservation properties, which is in accordance with the theoretical results.

https://doi.org/10.4208/aamm.2014.m888 Published online by Cambridge University Press



(a) (b)

Figure 4: The exact solution and numerical solution of the proposed schemes at $T=1$ for $\Delta t=0.01$, $h=1/4$, $c=0.8$, $x_0=0$. (a): energy-preserving scheme; (b): momentum-preserving scheme.



(a) (b)

Figure 5: Numerical errors of at $T=1$ for $\Delta t=0.01$, $h=1/4$, $c=0.8$, $x_0=0$. (a): energy-preserving scheme; (b): momentum-preserving scheme.

Remark 5.1. Here, for simplicity, we only present the numerical solution of the energy-preserving scheme. In fact, the other schemes have similar results. Combining the above observations, we think that the energy-preserving scheme is a better choice in practical computation.

5.2 Interaction of two solitary waves

In this example, we study the interaction of two solitary waves. The initial condition is given by

$$u(x,0)=\sqrt{6c_1}\operatorname{sech}\big(A_1(x-x_1)\big)+\sqrt{6c_2}\operatorname{sech}\big(A_2(x-x_2)\big),$$

https://doi.org/10.4208/aamm.2014.m888 Published online by Cambridge University Press

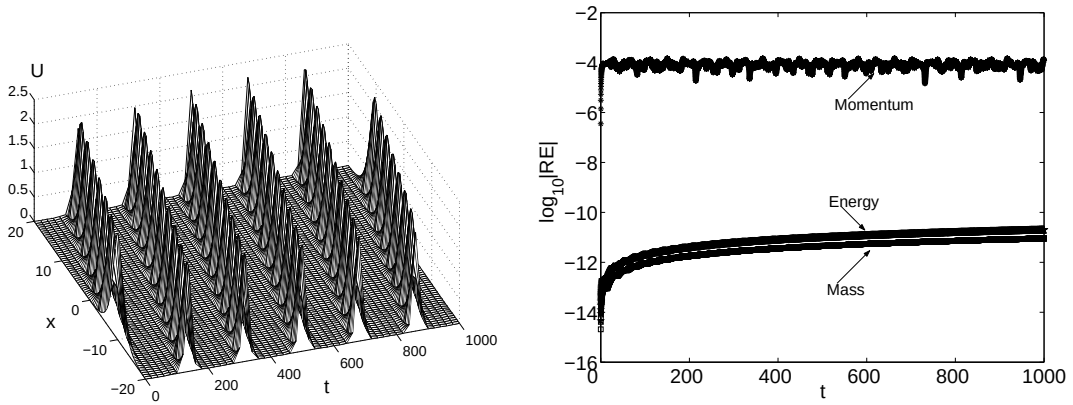


Figure 6: The numerical results of energy-preserving scheme with $T=1000$, $\Delta t=0.1$, $h=1/4$, $c=0.8$, $x_0=10$. (a): the numerical solution at $T=1000$; (b): the relative errors of invariants at $T=1000$.

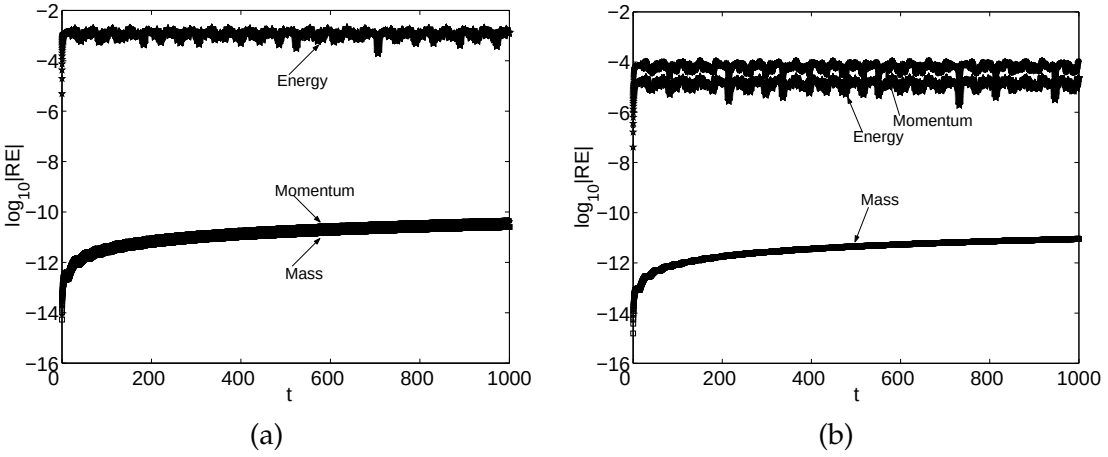
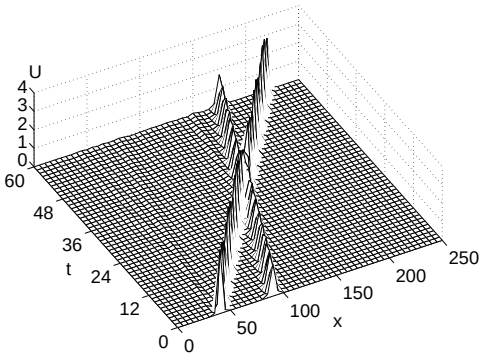


Figure 7: The relative errors of invariants for momentum-preserving scheme and finite volume element scheme with $T=1000$, $\Delta t=0.1$, $h=1/4$, $c=0.8$, $x_0=10$. (a): momentum-preserving scheme; (b): finite volume element scheme.

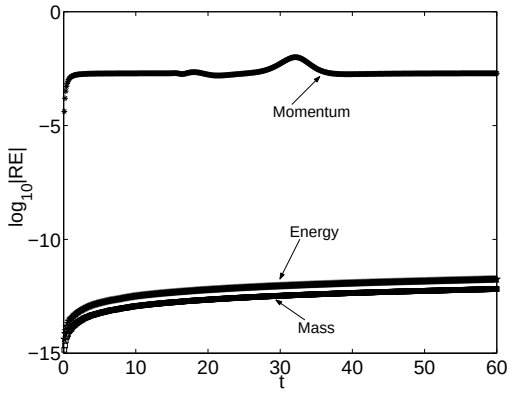
where $A_i=\sqrt{\frac{c_i}{c_i+1}}$, $i=1,2$, $x_1=40$, $x_2=90$, $c_1=2$, $c_2=0.5$. The first solitary wave is initially located at $x=x_1$ and moved to the right with speed c_1 and amplitude $\sqrt{6c_1}$. The other one is initially located at $x=x_2$ and moved to the right with the speed c_2 and amplitude $\sqrt{6c_2}$.

We perform a simulation with space step $h=1/2$ and time step $\Delta t=0.1$ for two solitary waves over the region $[0,250]$ up to time $T=60$. Fig. 8 presents the numerical results of the energy-preserving scheme in the time interval $[0,60]$. Fig. 8(a) presents the profile of two solitary waves and shows that the collision of the two solitary waves is elastic. Figs. 8(c)-

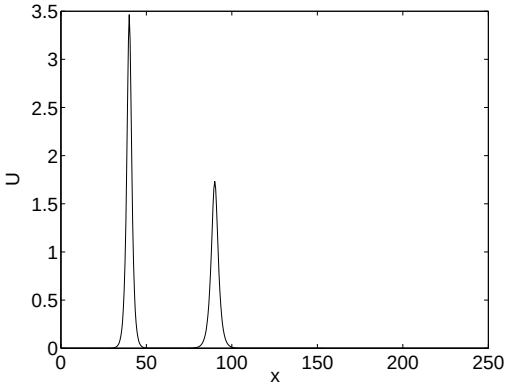
https://doi.org/10.4208/aamm.2014.m888 Published online by Cambridge University Press



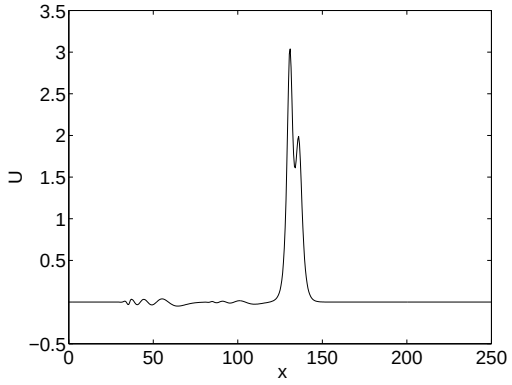
(a) The interaction of two solitary waves



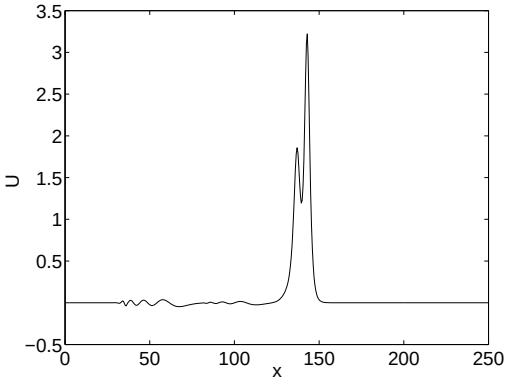
(b) The conservation properties of energy-preserving scheme



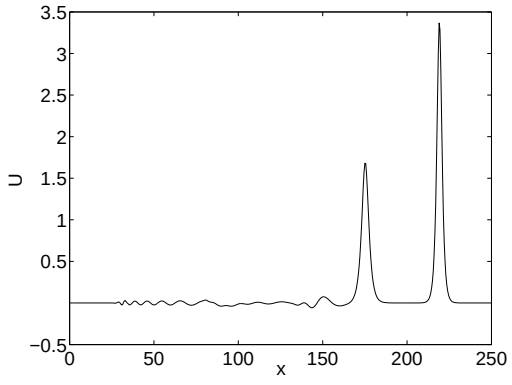
(c) The numerical solution at $T=0$



(d) The numerical solution at $T=30$



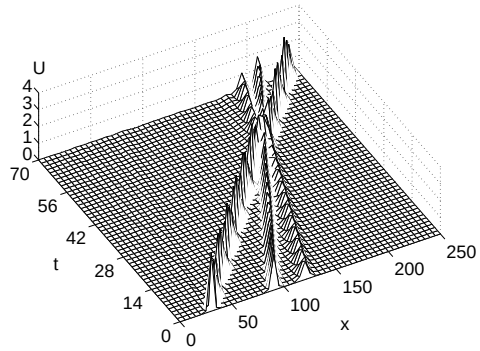
(e) The numerical solution at $T=34$



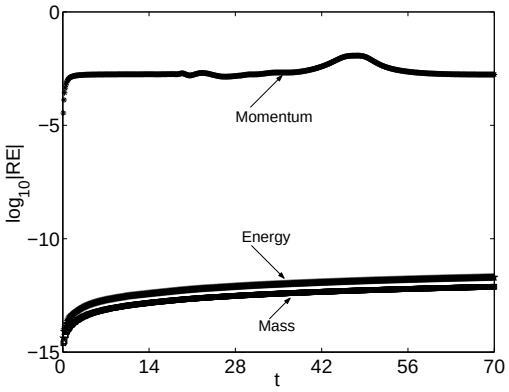
(f) The numerical solution at $T=60$

Figure 8: Computation for the two solitary waves initial state with $T=60$, $h=0.5$, $\Delta t=0.1$, $c_1=2$, $c_2=0.5$, $x_1=40$, $x_2=90$.

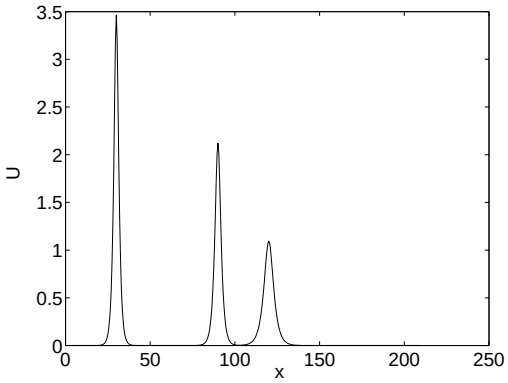
https://doi.org/10.4208/aamm.2014.m888 Published online by Cambridge University Press



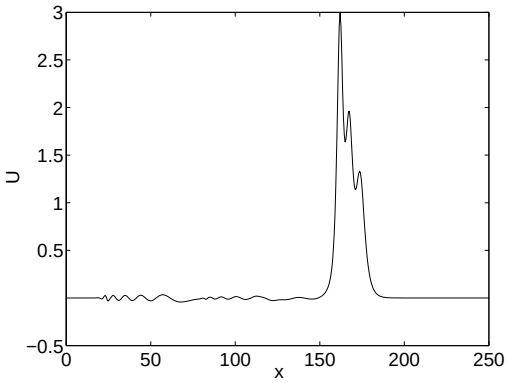
(a) The interaction of three solitary waves



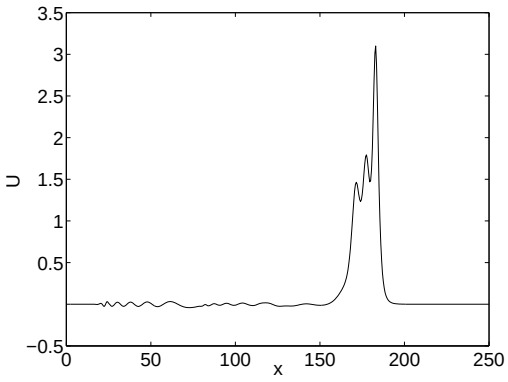
(b) The conservation properties of energy-preserving scheme



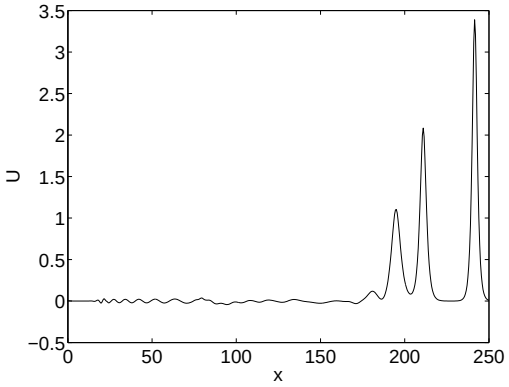
(c) The numerical solution at $T=0$



(d) The numerical solution at $T=45$



(e) The numerical solution at $T=50$



(f) The numerical solution at $T=70$

Figure 9: Computation for the three solitary waves initial state with $T=70$, $h=0.5$, $\Delta t=0.1$, $c_1=2$, $c_2=0.75$, $c_3=0.2$, $x_1=30$, $x_2=90$, $x_3=120$.

https://doi.org/10.4208/aamm.2014.m888 Published online by Cambridge University Press

8(f) present the numerical solution at different times and clearly show that the collision occurs at about $t=30$, and at about $t=34$, two solitary waves start to leave away. At about $t=60$, the two solitary waves fully leave away, and continue to propagate towards the right. It is noted that there produces small waves after collision. In addition, Fig. 8(b) presents the conservation properties of the energy-preserving scheme and shows that it can also precisely conserve the discrete mass and energy to within the machine precision.

5.3 Interaction of three solitary waves

In this example, we study the interaction of three solitary waves. The initial condition is given by

$$u(x,0)=\sum_{i=1}^{3}\sqrt{6c_i}\,\mathrm{sech}\big(A_i(x-x_i)\big),$$

where $A_i=\sqrt{\frac{c_i}{c_i+1}}$, $i=1,2,3$, $x_1=30$, $x_2=90$, $x_3=120$, $c_1=2$, $c_2=0.75$, $c_3=0.2$. The first solitary wave is initially located at $x=x_1$ and moved to the right with speed c_1 and amplitude $\sqrt{6c_1}$. The second one is initially located at $x=x_2$ and moved to the right with the speed c_2 and amplitude $\sqrt{6c_2}$. The third one is initially located at $x=x_3$ and moved to the right with the speed c_3 and amplitude $\sqrt{6c_3}$.

We perform a simulation with space step $h=1/2$ and time step $\Delta t=0.1$ for three solitary waves over the region $[0,250]$ up to time $T=70$. Fig. 9 presents the numerical results of the energy-preserving scheme in the time interval $[0,70]$. Fig. 9(a) presents the profile of three solitary waves and shows that the collision of the three solitary waves is also elastic. Figs. 9(c)-9(f) present the numerical solution at different times and clearly show that the collision occurs at about t=45, and the three solitary waves start leave away at about $t=50$. At about $t=70$, the three solitary waves fully leave away and continue to travel towards the right. It is noted that there also produces small waves after collision. In addition, Fig. 9(b) also presents the conservation properties of the energy-preserving scheme and shows that it can also precisely conserve the discrete mass and energy to within the machine precision.

6 Conclusions

In this paper, we propose three conservative finite volume element schemes for the nonlinear MRLW equation. Using the linear finite volume element method in space and symmetric scheme in time, we derive the energy-preserving scheme, momentum-preserving scheme and the classic finite volume element scheme. The numerical results show that the energy-preserving scheme have higher accuracy and better stability than the momentum-preserving scheme, and can correctly simulate the solitary wave behavior of the nonlinear MRLW equation, by preserving the mass and energy in the discrete level.

https://doi.org/10.4208/aamm.2014.m888 Published online by Cambridge University Press

Acknowledgements

This work is partially supported by the National Natural Science Foundation of China (Grant No. 11471166), Natural Science Foundation of Jiangsu Province (Grant No. BK20141443), Education Foundation for Young Teachers of Fujian Province (Grant No. JA14319), Undergraduate Technology Innovation Project in Fujian Province (Grant No. SJ2011019), Innovation Project for Graduate Education of Jiangsu Province (Grant No. KYLX15_0718) and the Priority Academic Program Development of Jiangsu Higher Education Institutions. On the other hand, the authors are very grateful to reviewers for carefully reading this paper and for their comments and suggestions.

References

[1] H. ZHANG, G.M. WEI AND Y. T. GAO, *On the general form of the Benjamin-Bona-Mahony equation in fluid mechanics*, Czechoslovak J. Phys., 52(3) (2002), pp. 373–377.
[2] S. B. G. KARAKOC, T. GEYIKLI AND A. BASHAN, *A numerical solution of the modified regularized long wave (MRLW) equation using quartic B-splines,* TWMS J. Eng. Math., 3(2) (2013), pp. 231–244.
[3] D. FURIHATA AND T. MATSUO, Discrete Variational Derivative Method: A Structure-Preserving Numerical Method for Partial Differential Equations, CRC Press, London, 2010.
[4] D. FURIHATA AND M. MORI, *A stable finite difference scheme for the Cahn-Hilliard equation based on a Lyapunov functional,* J. Appl. Math. Mech., 76(1) (1996), pp. 405–406.
[5] A. DURÁN AND M. A. LÓPEZ-MARCOS, *Conservative numerical methods for solitary wave interactions,* J. Phys. A. Math. Theor., 36(28) (2003), pp. 7761–7770.
[6] S. KOIDE AND D. FURIHATA, *Nonlinear and linear conservative finite difference schemes for regularized long wave equation,* Japan J. Indus. Appl. Math., 26(1) (2009), pp. 15–40.
[7] T. MATSUO AND D. FURIHATA, *Dissipative or conservative finite difference schemes for complex-valued nonlinear partial differential equations,* J. Comput. Phys., 171(2) (2001), pp. 425–447.
[8] T. YAGUCHI, T. MATSUO AND M. SUGIHARA, *An extension of the discrete variational method to nonuniform grids,* J. Comput. Phys., 229(11) (2010), pp. 4382–4423.
[9] T. MATSUO AND H. KURAMAE, *An alternating discrete variational derivative method,* AIP Conference Proceedings, 1479(1) (2012), pp. 1260–1263.
[10] H. KURAMAE AND T. MATSUO, *An alternating discrete variational derivative method for coupled partial differential equations,* Japan Soc. Indus. Appl. Math. Lett., 4 (2012), pp. 29–32.
[11] R. E. BANK AND D. J. ROSE, *Some error estimates for the box methods,* SIAM J. Numer. Anal., 24(4) (1987), pp. 777–787.
[12] W. HACKBUSCH, *On first and second order box schemes,* Computing, 41(4) (1989), pp. 277–296.
[13] R. H. LI, Z. Y. CHEN AND W. WU, Generalized Difference Methods for Differential Equations: Numerical Analysis of Finite Volume Methods, Marcel Dekker Inc., New York, 2000.
[14] Y. LI AND R. H. LI, *Generalized difference methods on arbitrary quadrilateral networks,* J. Comput. Math., 17(6) (1999), pp. 653–672.
[15] Q. X. WANG, Z. Y. ZHANG, X. H. ZHANG AND Q. Y. ZHU, *Energy-preserving finite volume element method for the improved Boussinesq equation,* J. Comput. Phys., 270 (2014), pp. 58–69.
[16] Z. Y. ZHANG, *Error estimates of finite volume element method for the pollution in groundwater flow,* Numer. Methods Partial Differential Equations, 25(2) (2009), pp. 259–274.

https://doi.org/10.4208/aamm.2014.m888 Published online by Cambridge University Press

[17] J. C. Xu and Q. S. Zou, *Analysis of linear and quadratic simplicial finite volume methods for elliptic equations,* Numerische Mathematik, 111(3) (2009), pp. 469–492.
[18] Z. Y. Zhang and F. Q. Lu, *Quadratic finite volume element method for the improved Boussinesq equation,* J. Math. Phys., 53(1) (2012), 013505.
[19] D. Dutykh, D. Clamond, P. Milewski and D. Mitsotakis, *Finite volume and pseudo-spectral schemes for the fully nonlinear 1D Serre equations,* Euro. J. Appl. Math., 24(5) (2013), pp. 761–787.
[20] D. Dutykh, Th. Katsaounis and D. Mitsotakis, *Finite volume methods for unidirectional dispersive wave models,* Int. J. Numer. Methods Fluids, 71(6) (2013), pp. 717–736.
[21] S. Li and L. Vu-Quoc, *Finite difference calculas invariant structure of a class of algorithms for the nonlinear Klein-Gordon equation,* SIAM J. Numer. Anal., 32(6) (1995), pp. 1839–1875.
[22] L. R. T. Gardner, G. A. Gardner, F. A. Ayoub and N. K. Amein, *Approximations of solitary waves of the MRLW equation by B-spline finite element,* Arabian J. Sci. Eng. A Sci., 22(2) (1997), pp. 183–193.
[23] A. K. Khalifa, K. R. Raslan and H. M. Alzubaidi, *A collocation method with cubic B-splines for solving the MRLW equation,* J. Comput. Appl. Math., 212(2) (2008), pp. 406–418.
[24] A. K. Khalifa, K. R. Raslan and H. M. Alzubaidi, *A finite difference scheme for the MRLW and solitary wave interactions,* Appl. Math. Comput., 189(1) (2007), pp. 346–354.
[25] K. R. Raslan, *Numerical study of the modified regularized long wave equation,* Chaos, Solitons and Fractals, 42(3) (2009), pp. 1845–1853.
[26] J. X. Cai, *A multisymplectic explicit scheme for the modified regularized long-wave equation,* J. Comput. Appl. Math., 234(3) (2010), pp. 899–905.
[27] M. A. Johnson, *On the stability of periodic solutions of the generalized Benjamin-Bona-Mahony equation,* Physica D: Nonlinear Phenomena, 239(19) (2010), pp. 1892–1908.
[28] P. J. Olver, *Euler operators and conservation laws of the BBM equation,* Mathematical Proceedings of the Cambridge Philosophical Society, 85(1) (1979), pp. 143–160.
[29] N. Yi, Y. Huang and H. Liu, *A direct discontinuous Galerkin method for the generallized Korteweg-de Vries equation: energy conservation and boundary effect,* J. Comput. Phys., 242 (2013), pp. 351–366.
[30] M. Dahlby and O. Brynjulf, *A general framework for deriving integral preserving numerical methods for PDEs,* SIAM J. Sci. Comput., 33(5) (2011), pp. 2318–2340.
[31] Y. Z. Gong, J. X. Cai and Y. S. Wang, *Some new structure-preserving algorithms for general multi-symplectic formulations of Hamiltonian PDEs,* J. Comput. Phys., 279 (2014), pp. 80–102.
[32] H. C. Li, J. Q. Sun and M. Z. Qin, *Multi-symplectic method for the Zakharov-Kuznetsov equation,* Adv. Appl. Math. Mech., 7(1) (2015), pp. 58–73.

https://doi.org/10.4208/aamm.2014.m888 Published online by Cambridge University Press